

Platinum(II) complexes with bidentate iminopyridine ligands: Synthesis, spectral characterization, properties and structural analysis

Saeed Dehghanpour^{a,*}, Ali Mahmoudi^b, Soghra Rostami^b

^a Department of Chemistry, Alzahra University, P.O. Box 1993891176, Tehran, Iran

^b Department of Chemistry, Islamic Azad University, Karaj Branch, Karaj, Iran

ARTICLE INFO

Article history:

Received 21 December 2009

Accepted 13 April 2010

Available online 28 April 2010

Keywords:

Platinum(II) complexes

Diimine ligands

Spectroscopy

Electrochemistry

Crystal structures

ABSTRACT

Four platinum(II) complexes, [PtCl₂L] (L = (4-fluorophenyl)pyridin-2-ylmethylene-amine, **1**; (4-chlorophenyl)pyridin-2-ylmethyleneamine, **2**; (4-bromophenyl)pyridin-2-ylmethyleneamine, **3** and (4-iodophenyl)pyridin-2-ylmethyleneamine, **4**) have been synthesized and characterized by CHN analysis, IR and UV–Vis spectroscopy. The crystal structures of **1** and **2** were determined using single crystal X-ray diffraction. The coordination polyhedron about the platinum (II) center in the complexes is best described as distorted square planar. The complexes undergo stacking to form a zigzag Pt...Pt...Pt chain containing both short (3.57(7) Å in **1** and 3.62(8) Å in **2**) and long (5.16(7) Å in **1** and 5.41(9) Å in **2**) Pt...Pt separations through the crystal. The compounds absorb moderately in the visible region, owing to a charge-transfer-to-diimine electronic transition. The redox potentials are approximately insensitive to the substituents on the phenyl ring of the ligands.

© 2010 Elsevier Ltd. All rights reserved.

1. Introduction

Platinum complexes with the diimine ligands have inspired considerable research efforts. For example, such complexes have found widespread use as optical materials, DNA intercalators and solar cell dyes [1–5]. The interesting photochemical and photo-physical properties of such compounds have also been thoroughly investigated [6,7]. Factors such as steric, electronic and conformational interactions influence the spectroscopic properties of these complexes and modify their redox potentials, which are important in practical applications [8–10]. The majority of research in this field has focused on the use of polypyridine derivatives such as 2,2'-bipyridine, 1,10-phenanthroline as ligands [11–14]. However, there is little data on complexes with unsymmetrical diimine ligands containing iminopyridine [15–18]. According to this view, we describe the synthesis, properties and structural characterization of Pt(II) complexes of the type [PtCl₂L₂] in which L is an unsymmetrical bidentate iminopyridine ligand.

2. Experimental

2.1. General

All chemicals used were reagent grade and were used as received. Solvents used for the reactions were purified by literature

methods [19]. Samples of [PtCl₂(CH₃CN)₂] were prepared as described in the literature [20]. The ligands (4-fluorophenyl)pyridin-2-ylmethylene-amine, **A**, (4-chlorophenyl)pyridin-2-ylmethyleneamine, **B**, (4-bromophenyl)pyridin-2-ylmethyleneamine, **C**, and (4-iodophenyl)pyridin-2-ylmethyleneamine, **D** were prepared according to reported procedures [21]. Elemental analyses were performed using a Heraeus CHN-O-RAPID elemental analyzer. Infrared spectra were recorded on a Bruker Tensor 27 instrument. Electronic absorption spectra were recorded on a JASCO V-570 spectrophotometer; λ_{max} (log ε). NMR spectra were obtained on a BRUKER AVANCE DRX500 (500 MHz) spectrometer. Proton chemical shifts are reported in parts per million (ppm) relative to an internal standard of Me₄Si. All Pt chemical shifts are reported in parts per million (ppm) relative to K₂PtCl₄. All voltammograms were recorded using a three electrode system consisting of an Ag/AgCl reference electrode, a platinum wire counter electrode and an Au working electrode. A Metrohm multipurpose instrument model 693 VA processor with 694A Va stand was used. In all electrochemical experiments, the test solutions were purged with argon gas for at least 5 min.

2.2. Syntheses

2.2.1. Synthesis of PtCl₂(A), **1**

Although complexes **1** and **2** have been synthesized before [22,23], here we report a new method for their synthesis. A 125 ml Schlenk flask equipped with a magnetic stirring bar was charged with PtCl₂(CH₃CN)₂ (35.0 mg, 0.1 mmol) and 20 mg

* Corresponding author. Tel./fax: +98 21 88041344.

E-mail address: dehghanpour_farasha@yahoo.com (S. Dehghanpour).

(0.1 mmol) (4-fluorophenyl)pyridin-2-ylmethyleneamine, **A** and flushed with nitrogen. Acetonitrile (20 ml) was added using a syringe and the resulting solution was sealed under nitrogen, heated to 50 °C, and stirred for 48 h to complete the transformation to the desired product. The solid precipitating from the solution upon cooling to ambient temperature was isolated by filtration and washed with acetonitrile. The precipitate was dissolved in chloroform (4 ml). Blowing diethyl ether vapor into the solution gave orange crystals, which were filtered off and washed with diethyl ether and dried at reduced pressure. Yield: 81%. IR (KBr/*v*, cm⁻¹): 1595 (C=N). ¹H NMR (DMSO-d₆, ppm): 7.30–7.54 (m, 3H, ArH, amine ring), 7.98 (t, 1H, *J*_{H1,2} = 5.6, *J*_{H2,3} = 7.3, H2), 8.21 (d, 1H, *J*_{H4,3} = 8.1, H4), 8.43 (t, 1H, *J*_{H3,2} = 7.3, *J*_{H3,4} = 8.1, H3), 9.33 (s, 1H, *J*_{pt-H} = 47, H5), 9.46 (d, 1H, *J*_{H2,1} = 5.6, *J*_{pt-H} = 32, H1). ¹⁹⁵Pt NMR (DMSO-d₆, ppm): –2212. *Anal. Calc.* for C₁₂H₉Cl₂FN₂Pt: C, 30.92; H, 1.95; N, 6.01. Found: C, 30.85; H, 1.92; N, 6.09%.

2.2.2. Synthesis of PtCl₂(B), **2**

This complex was prepared by a procedure similar to **1** using 21.7 mg (0.1 mmol) of (4-chlorophenyl)pyridin-2-ylmethyleneamine, **B**. Orange crystals of **2** suitable for single crystal X-ray diffraction were isolated directly from the solution after a few days. As the crystals slowly deteriorated on standing, presumably due to loss of solvent, samples for microanalyses were dried *in vacuo*. Yield: 79%. IR (KBr/*v*, cm⁻¹): 1586 (C=N). ¹H NMR (DMSO-d₆, ppm): 7.36–7.54 (m, 3H, ArH, amine ring), 7.98 (t, 1H, *J*_{H1,2} = 5.7, *J*_{H2,3} = 6.4, H2), 8.21 (d, 1H, *J*_{H4,3} = 9.1, H4), 8.44 (t, 1H, *J*_{H3,2} = 6.4, *J*_{H3,4} = 9.1, H3), 9.32 (s, 1H, *J*_{pt-H} = 45, H5), 9.47 (d, 1H, *J*_{H2,1} = 5.7, *J*_{pt-H} = 31, H1). ¹⁹⁵Pt NMR (DMSO-d₆, ppm): –2211. *Anal. Calc.* for C₁₂H₉Cl₂FN₂Pt: C, 29.86; H, 1.88; N, 5.80. Found: C, 29.92; H, 1.85; N, 5.74%.

2.2.3. Synthesis of PtCl₂(C), **3**

This complex was prepared by a procedure similar to that for the synthesis of **1** using 26.1 mg (0.1 mmol) of (4-bromophenyl)pyridin-2-ylmethyleneamine, **C**. Orange crystals were collected

by filtration and dried *in vacuo*. As the crystals slowly deteriorated on standing, presumably due to loss of solvent, samples for microanalyses were dried *in vacuo*. Yield: 79%. IR (KBr/*v*, cm⁻¹): 1580 (C=N). ¹H NMR (DMSO-d₆, ppm): 7.42–7.71 (m, 3H, ArH, amine ring), 7.99 (t, 1H, *J*_{H1,2} = 5.7, *J*_{H2,3} = 6.5, H2), 8.22 (d, 1H, *J*_{H4,3} = 7.9, H4), 8.44 (t, 1H, *J*_{H3,2} = 6.5, *J*_{H3,4} = 7.9, H3), 9.34 (s, 1H, *J*_{pt-H} = 44, H5), 9.45 (d, 1H, *J*_{H2,1} = 5.7, *J*_{pt-H} = 31, H1). ¹⁹⁵Pt NMR (DMSO-d₆, ppm): –2209. *Anal. Calc.* for C₁₂H₉Cl₂FN₂Pt: C, 27.34; H, 1.72; N, 5.31. Found: C, 27.38; H, 1.79; N, 5.26%.

2.2.4. Synthesis of PtCl₂(D), **4**

This complex was prepared by a procedure similar to that for the synthesis of **1** using 30.8 mg (0.1 mmol) of (4-iodophenyl)pyridin-2-ylmethyleneamine, **D**. Orange crystals were collected by filtration and dried *in vacuo*. Yield: 79%. IR (KBr/*v*, cm⁻¹): 1575 (C=N). ¹H NMR (DMSO-d₆, ppm): 7.27–7.87 (m, 3H, ArH, amine ring), 7.98 (t, 1H, *J*_{H1,2} = 5.6, *J*_{H2,3} = 6.1, H2), 8.22 (d, 1H, *J*_{H4,3} = 9.1, H4), 8.43 (t, 1H, *J*_{H3,2} = 6.1, *J*_{H3,4} = 9.1, H3), 9.32 (s, 1H, *J*_{pt-H} = 46, H5), 9.46 (d, 1H, *J*_{H2,1} = 5.6, *J*_{pt-H} = 33, H1). ¹⁹⁵Pt NMR (DMSO-d₆, ppm): –2206. *Anal. Calc.* for C₁₂H₉Cl₂FN₂Pt: C, 25.11; H, 1.58; N, 4.88. Found: C, 25.16; H, 1.62; N, 4.89%.

2.3. X-ray analyses

Data were collected on a Bruker-Nonius Kappa-CCD diffractometer using monochromated Mo K α radiation and measured using a combination of ϕ scans and ω scans with κ offsets to fill the Ewald sphere. The data was processed using the Denzo-SMN package [24]. Absorption corrections were carried out using SORTAV [25]. The structures were solved and refined using SHELXTL V6.1 [26] for full-matrix least-squares refinement based on F^2 . All H-atoms were included in calculated positions and allowed to refine in a riding-motion approximation with U_{iso} tied to the carrier atom. Crystallographic data for the compounds are given in Table 1.

Table 1

Crystal data and single crystal X-ray diffraction refinement details for compounds **1** and **2**·1/4CH₃CN.

	C ₁₂ H ₉ Cl ₂ FN ₂ Pt	C _{12.50} H _{9.75} Cl ₃ N _{2.25} Pt
Empirical formula	C ₁₂ H ₉ Cl ₂ FN ₂ Pt	C _{12.50} H _{9.75} Cl ₃ N _{2.25} Pt
Formula weight	466.20	492.92
Temperature (K)	150(1)	150(2)
Wavelength (Å)	0.71073	0.71073
Crystal system	monoclinic	monoclinic
Space group	P2/n	C2/c
<i>a</i> (Å)	7.5531(6)	35.2284(15)
<i>b</i> (Å)	12.1563(10)	7.6261(4)
<i>c</i> (Å)	13.9331(7)	26.0259(9)
β (°)	101.466(5)	127.465(2)
<i>V</i> (Å ³)	1253.77(16)	5549.7(4)
<i>Z</i>	4	16
Density (g cm ⁻³)	2.470	2.360
μ (mm ⁻¹)	11.610	10.675
<i>F</i> (0 0 0)	864	3672
Crystal size	0.17 × 0.07 × 0.03	0.08 × 0.04 × 0.03
Theta range for data collection	2.86–24.99	2.77–25.00
Index ranges	–8 ≤ <i>h</i> ≤ 8, –14 ≤ <i>k</i> ≤ 14, –16 ≤ <i>l</i> ≤ 16	–41 ≤ <i>h</i> ≤ 41, –9 ≤ <i>k</i> ≤ 9, –30 ≤ <i>l</i> ≤ 30
Reflections collected	6907	21,665
Independent reflections	2186 [<i>R</i> _{int} = 0.0609]	4862 [<i>R</i> _{int} = 0.1323]
Completeness to theta = 25.00°	99.9%	99.7%
Absorption correction	semi-empirical from equivalents	semi-empirical from equivalents
Max. and min. transmission	0.654 and 0.345	0.740 and 0.495
Refinement method	full-matrix least-squares on F^2	full-matrix least-squares on F^2
Data/restraints/parameters	2186/0/163	4862/48/340
Goodness-of-fit (GOF) on F^2	1.045	1.030
Final <i>R</i> indices [<i>I</i> > 2 σ (<i>I</i>)]	<i>R</i> ₁ = 0.0545, <i>wR</i> ₂ = 0.1417	<i>R</i> ₁ = 0.0539, <i>wR</i> ₂ = 0.1070
<i>R</i> indices (all data)	<i>R</i> ₁ = 0.0669, <i>wR</i> ₂ = 0.1554	<i>R</i> ₁ = 0.1150, <i>wR</i> ₂ = 0.1350
Largest differences in peak and hole (e Å ⁻³)	3.719 and –2.785	2.920 and –1.964

Table 2
UV–Vis spectral data and cyclic voltammetric data of the complexes.

Compound	λ_{\max}/nm , $\log \epsilon/\text{M}^{-1} \text{cm}^{-1\text{a}}$	Reduction ^b		Oxidation ^b
		$E_{\text{pc1}}(i_{\text{pc}}/i_{\text{pa}})$	E_{pc2}	E_{pa}
1	423(2.64), 336(3.13), 266(3.79), 260(3.79)	–1.13(0.3)	–1.70	0.67
2	425(2.38), 319(2.91), 267(3.25), 259(3.26)	–1.12(0.2)	–1.75	0.65
3	423(2.68), 334(3.24), 283(3.46), 259(3.56)	–1.14(0.3)	–1.76	0.64
4	424(2.72), 339(3.38), 283(3.56), 259(3.76)	–1.12(0.2)	–1.74	0.68

^a Solvent: DMSO.

^b Solvent: CH₃CN, scan rate = 0.1 V s^{–1}.

3. Results and discussion

3.1. Synthesis and spectral properties

The reaction of the ligands with [PtCl₂(CH₃CN)₂] yields the complexes [PtCl₂(L)₂]. These complexes are orange solids, which are soluble in chloroform, methanol, ethanol, and acetone and are stable under ambient conditions. Although Kawakami et al. described the synthesis of complex **1** with (C₆H₅CN)PtCl₂ as the starting material, there is no clear NMR data of the complex due to the low intensity of the signals. However, using the M–Cl bands observed in the infrared spectrum, a square planar geometry was concluded for the complex (which is in accord with the X-ray analysis report in this paper) [22]. The synthesis of complex **1** was also reported by Scale and co-workers. The precursor complex was PtCl₂(coe)₂ and cytotoxic properties, ¹H, ¹³C and ¹⁹F NMR data of the complex have been reported [23].

Elemental analysis confirms the named stoichiometries of all the complexes. The IR spectra in the 4000–400 cm^{–1} range show that the ligand is coordinated to the Pt(II) ions. The most striking bands of the diimine ligands ($\nu(\text{C}=\text{N})$) decrease in frequency when they are part of the complexes [21,27].

The peak assignments for the ¹H NMR spectra are presented in the experimental section for each complex. These peaks are assigned based on the splitting of the resonance signals, spin coupling constants, literature data and in accordance with the molecular structure determined by the X-ray crystal structure analysis. The ¹H resonances of the coordinated ligands are observed in complexes **1–4**. Aside from the aromatic H-atoms, which appear at 7.27–7.87 ppm, the imine protons appear as a singlet at 9.32–9.34 ppm. The downfield shift of the imine protons relative to the free ligands can be attributed to the deshielding effect resulting from the coordination of the metal by the ligands [9]. Platinum satellites are also observed for this resonance ($J_{\text{H-Pt}} \sim 45$ Hz) upon complexation of the ligand with the metal. Similar trends are also observed for the ortho proton of the pyridine ring as the chemical shift changes from δ 9.45 to 9.47 ppm ($J_{\text{H-Pt}} \sim 32$ Hz). The other protons of the pyridine ring appear at 7.98–8.44 ppm and the assignments are given in the experimental section. The ¹⁹⁵Pt NMR spectra of the platinum Schiff base complexes show signals at –2212 ppm for **1**, –2211 ppm for **2**, –2209 ppm for **3** and –2206 ppm for **4**. The data is consistent with a platinum environment of two nitrogens and two chlorines [28–31].

The electronic spectra of the complexes were recorded in the 700–200 nm range. The spectral data is presented in Table 2. The uncoordinated ligands are completely transparent above 335 nm

[21]. The absorption spectra of all the complexes exhibit a broad band close to 425 nm. This lowest energy feature in each case is the metal-to-ligand (Pt_{II} → imine π^*) charge transfer (MLCT) transition. A slight red-shift of this band with an increase in the dipole moment of the solvent can be noted (Table 3). A similar shift has been reported for complexes of the type [Pt(NN)Cl₂] [8,32,33]. Other higher energy bands are observed, which are combinations of internal $\pi-\pi^*$ transitions and higher energy MLCT transitions.

The redox behavior of the complexes in CH₃CN solution was examined by cyclic voltammetry. In general, these complexes show two reduction waves at potentials ranging from –1.75 to –1.12 V (Fig. 1). The first reduction wave is quasireversible and the ratio of the anodic and cathodic peak currents, $i_{\text{pa}}/i_{\text{pc}}$, approaches 1 as the scan rate increases. The peak-to-peak separation for the first reduction wave varies from 120 to 180 mV as the scan rate is changed from 50 to 700 mV/s. The second reduction wave is irreversible in acetonitrile, showing no anodic peak. The corresponding anodic peak is not observed even under fast-scan-rate conditions. This is probably due to an irreversible chemical reaction (due to the instability of the reduction products) following the electron-transfer process. A similar reduction wave is also observed in structurally related complexes [34,35]. A similar difference between the first and the second reduction potential is consistent with those found for similar complexes with the same electrochemical process [8,32,34–36]. An irreversible oxidation is observed in the anodic region for complexes **1–4** at about +0.67 V, which can be assigned to platinum [8,32,34–36]. No significant changes are observed with variation of the ligands in the oxidation wave of the complexes.

3.2. Crystal structures

The crystallographic data for compounds **1** and **2** are summarized in Table 1 and selected bond distances and angles are given in Table 4.

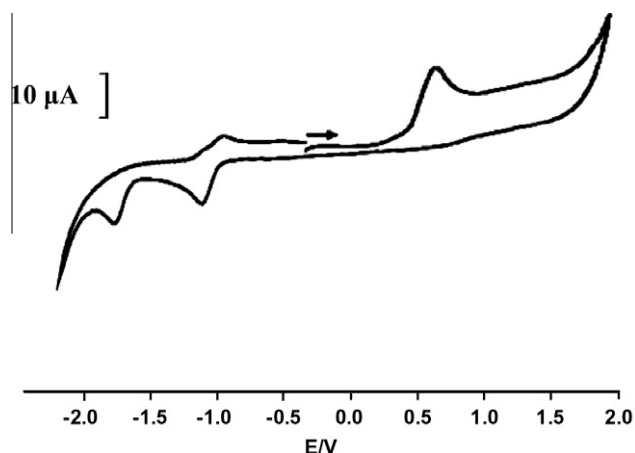


Fig. 1. Cyclic voltammograms of **1** in acetonitrile at 25 °C, [Bu₄N]ClO₄ supporting electrolyte (0.1 M), scan rate = 0.10 V s^{–1}.

Table 3
Effect of solvents on the low-energy MLCT band of complexes **1–4**.

	CHCl ₃	CH ₃ CN	DMF	DMSO
1	412	415	418	423
2	414	416	420	425
3	4.10	414	416	423
4	415	418	421	424

Table 4
Selected bond lengths [Å] and bond angles [°] for **1** and **2**·1/4CH₃CN.

1	2 CH ₃ CN				
	I		II		
Pt(1)–N(1)	2.017(11)	Pt(1A)–N(1A)	2.007(11)	Pt(1B)–N(1B)	2.030(10)
Pt(1)–N(2)	2.027(10)	Pt(1A)–N(2A)	2.014(10)	Pt(1B)–N(2B)	2.032(10)
Pt(1)–Cl(1)	2.288(3)	Pt(1A)–Cl(2A)	2.285(3)	Pt(1B)–Cl(1B)	2.289(4)
Pt(1)–Cl(2)	2.299(3)	Pt(1A)–Cl(1A)	2.299(4)	Pt(1B)–Cl(2B)	2.289(3)
N(1)–Pt(1)–N(2)	80.1(4)	N(1A)–Pt(1A)–N(2A)	79.5(4)	N(1B)–Pt(1B)–N(2B)	80.7(4)
N(1)–Pt(1)–Cl(1)	94.7(3)	N(1A)–Pt(1A)–Cl(2A)	175.6(3)	N(1B)–Pt(1B)–Cl(1B)	93.5(3)
N(2)–Pt(1)–Cl(1)	174.8(3)	N(2A)–Pt(1A)–Cl(2A)	97.1(3)	N(2B)–Pt(1B)–Cl(1B)	174.2(3)
N(1)–Pt(1)–Cl(2)	175.6(3)	N(1A)–Pt(1A)–Cl(1A)	94.7(4)	N(1B)–Pt(1B)–Cl(2B)	177.6(3)
N(2)–Pt(1)–Cl(2)	96.6(3)	N(2A)–Pt(1A)–Cl(1A)	174.2(3)	N(2B)–Pt(1B)–Cl(2B)	98.0(3)
Cl(1)–Pt(1)–Cl(2)	88.56(11)	Cl(2A)–Pt(1A)–Cl(1A)	88.67(13)	Cl(1B)–Pt(1B)–Cl(2B)	87.75(13)

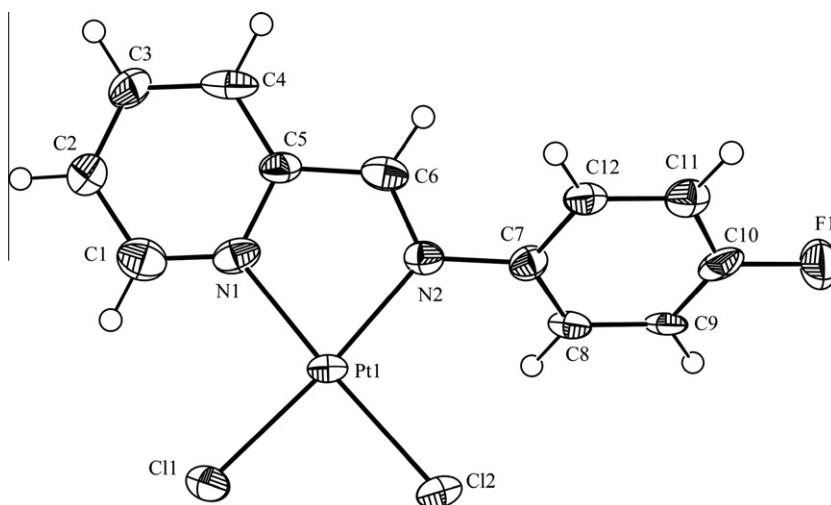


Fig. 2. Structure of **1** in the crystal, showing the atom-labelling scheme and thermal ellipsoids with 50% probability.

3.2.1. [Pt(A)Cl₂] (**1**)

A view of complex **1**, including the atom numbering scheme, is illustrated in Fig. 2. The geometry around the d⁸ Pt center in **1** is a distorted square plane, where the relatively small N(1)–Pt–N(2) bond angle of 80.51(8)° is a result of chelating ligand steric constraints. The bond angles around the Pt atom are consistent with a planar geometry, which sum to 359.96°. All of the Pt–N and Pt–Cl bond lengths and angles are very similar to those previously reported in related systems [14,15]. The relatively short C=N bond length of 1.284(16) Å for C(6)–N(2), compared to the C(1)–N(1) bond length of 1.329(17) Å and the C(5)–N(1) bond length of 1.369(18) Å in the pyridine ring, is consistent with a lack of imine double-bond delocalization in **1** [15].

A mean plane analysis of the five atoms comprising the transition metal square plane reveals a maximum deviation from ideality of 0.095(12) Å for N(1). In addition, a least-squares analysis of the 11 atoms, including those in the pyridine and the metal chelate rings, finds a maximum deviation of only 0.2614(114) Å for C(4). The aryl ring of the pyridinylimine ligand, containing C(7)–C(12), is tilted out-of-plane with respect to the metal chelate plane, with a calculated torsion angle of 42.64(6)° between the two planes. Terminal phenyl rings which contain bulkier non-hydrogen substituents tend to adopt a nearly perpendicular position relative to the metal chelation plane in structurally related compounds [37–40]. The molecules stack in the *a* direction in a head to tail fashion with two different Pt...Pt distances (Fig. 3). In this arrangement, the short Pt...Pt distance is 3.57(7) Å. The second Pt...Pt distance is much longer (5.16(7) Å) and the Pt...Pt...Pt chain angle is 118.66(2)°. The platinum–platinum vector in **1** inclines by only

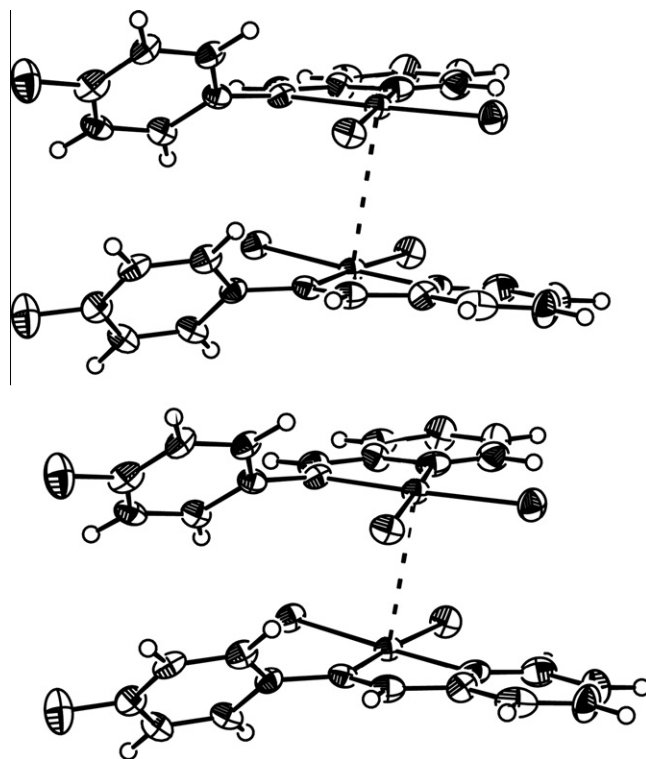


Fig. 3. Crystal packing of **1**, the stacking occurs along the *a*-axis.

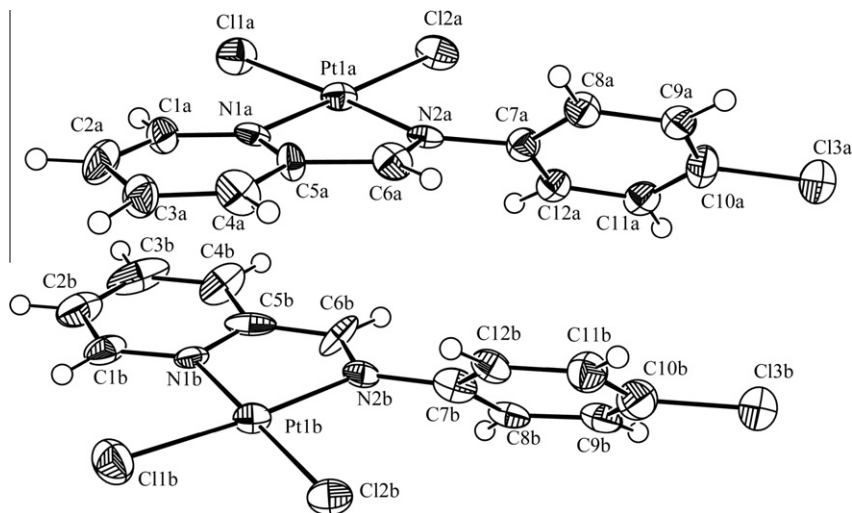


Fig. 4. Structure of 2·1/4CH₃CN in the crystal, showing the atom-labelling scheme and thermal ellipsoids with 50% probability.

Table 5
Geometry of the pyridine, chelate and benzene ring in compounds **1** and **2**.

	1	2	
		A	B
Planes 1 (pyridine ring)	N1–C1–C2–C3–C4–C5	N1a–C1a–C2a–C3a–C4a–C5a	N1b–C1b–C2b–C3b–C4b–C5b
Planes 2 (chelate ring)	N1–C5–C6–N2	N1a–C5a–C6a–N2a	N1b–C5b–C6b–N2b
Planes 3 (benzene ring)	C7–C8–C9–C10–C11–C12	C7a–C8a–C9a–C10a–C11a–C12a	C7b–C8b–C9b–C10b–C11b–C12b
Dihedral angle (°) between planes 1 and 2	2.596(5)	2.711(5)	1.505(5)
Dihedral angle (°) between planes 2 and 3	44.262(4)	49.723(5)	47.063(5)
Dihedral angle (°) between planes 1 and 3	42.644(5)	47.746(5)	45.754(6)
Torsion angle (°) N–C–C–N	–0.266(2)	–1.573(3)	–3.492(3)

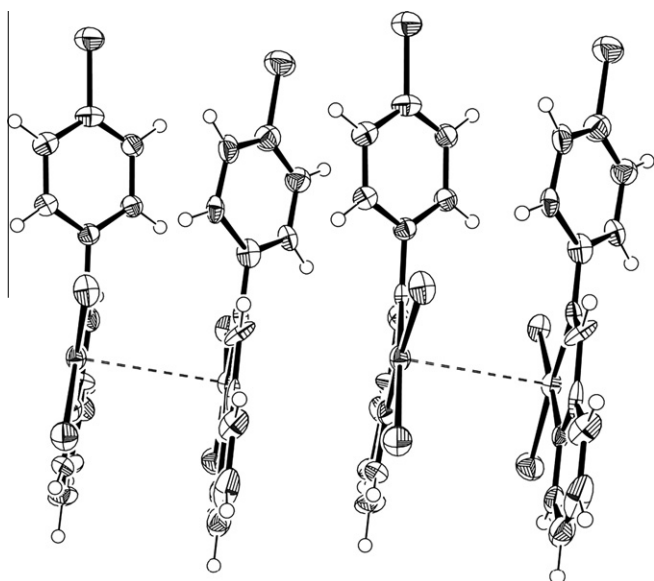


Fig. 5. Crystal packing of **2**, the stacking occurs along the *b*-axis.

13.08(11)° with respect to the perpendicular of the coordination plane, and the platinum atoms are not placed orthogonally on top of one another. Instead, they are shifted by 2.14(6) Å in the direction towards the ligand. Most of the reported values for Pt...Pt interactions are in the range 3.09–3.40 Å [13,18,41]. The Pt...Pt separation is too long to support a significant metal–metal interaction.

Although the molecules stack in the *a* direction in a head to tail fashion, the phenyl rings of the ligands are on one side and are approximately parallel to each other. Therefore, there is partial overlapping between these moieties with a nearest distance of 3.35 Å between the parallel the planes.

3.2.2. [Pt(B)Cl₂].1/4CH₃CN (2·1/4CH₃CN)

Compound **2** crystallizes with two molecules per asymmetric unit (molecule A and B) showing some conformational differences (Fig. 4). The crystal structure of complex **2** consists of monomeric cis-[Pt(B)Cl₂] molecules. The Pt center has a typical square planar geometry in which the largest deviation from the mean coordination plane is 0.089(2) Å (in N1a) and –0.064(2) Å (in N1b), very similar to that of [Pt(A)Cl₂]. The average Pt–Cl and Pt–N bond lengths (2.020, 2.291 Å) can be regarded as normal compared with the distances reported in the literature (Pt–Cl: 2.281–2.311 Å and Pt–N: 1.998–2.014 Å) [8,14]. The N(1a)–Pt(1a)–N(2a) and N(1b)–Pt(1b)–N(2b) bite angles, 79.5(4) and 80.7(4)°, are similar to those found in **1** and structurally related compounds, e.g. [PtCl₂L] (L = pyridinecarboxaldehydes derivative) (79.79°) [14]. The values for the dihedral angles of N1a–C5a–C6a–N2a and N1b–C5b–C6b–N2b are –1.573(3)° and –3.492(3)°, and comparison of the dihedral angles between the chelate rings and pyridine groups (Table 5) indicates the coplanarity of these moieties. However, the ligand is not completely planar. The phenyl groups are slightly twisted with respect to these moieties. In the structure of **2**, the platinum–platinum vector is inclined by 14.15(9)° with respect to the coordination plane. The platinum atoms are shifted by 2.34(1) Å towards the ligand in the *a* direction. As a consequence, the molecules no longer overlap with the halogen ligands sandwiched between the chelate planes and vice versa, but there are partially

overlapping ligands with a nearest distance between the parallel pyridine planes of 3.09(2) Å. Again, the molecules stack in the *b* direction in a head to tail fashion with two different Pt...Pt distances (Fig. 5). In this arrangement, the short Pt...Pt distance is 3.62(8) Å. The second Pt...Pt distance is much longer (5.41(9) Å) and Pt...Pt...Pt chain angle is 113.91(2)°.

4. Conclusion

Four Pt complexes, [Pt(NN)Cl₂] (NN = (4-fluorophenyl)pyridin-2-ylmethyleneamine (**1**), (4-chlorophenyl)pyridin-2-ylmethyleneamine (**2**), (4-bromophenyl)pyridin-2-ylmethyleneamine (**3**), (4-iodophenyl)pyridin-2-ylmethyleneamine (**4**)) have been synthesized. The crystal structures of **1** and **2** reveal a distorted square planar configuration. The aryl ring of the pyridinylimine ligands in **1** and **2** are tilted out-of-plane with respect to the metal chelate plane, with an average torsion angle of 47.01° between the two planes. All of these complexes exhibit low-energy absorption bands at about 424 nm, corresponding to a MLCT transition. In general, these complexes show two reduction waves at potentials ranging from –1.75 to –1.12 V. An irreversible oxidation is also observed in the anodic region for complexes **1–4** at about +0.67 V. However, the potentials and absorption bands are insensitive to the substituent on the phenyl ring of the iminopyridine ligands.

5. Supplementary data

CCDC 753586 and 753586 contain the supplementary crystallographic data for this paper. These data can be obtained free of charge via <http://www.ccdc.cam.ac.uk/conts/retrieving.html>, or from the Cambridge Crystallographic Data Centre, 12 Union Road, Cambridge CB2 1EZ, UK; fax: (+44) 1223-336-033; or e-mail: deposit@ccdc.cam.ac.uk.

Acknowledgment

Financial support by Alzahra University is gratefully acknowledged.

References

- [1] J.A. Weinstein, M.T. Tierney, E.S. Davies, K. Base, A.A. Robeiro, M.W. Grinstaff, *Inorg. Chem.* 42 (2003) 4544.
- [2] W.H. Chen, E.W. Reinheimer, K.R. Dunbar, M.A. Omary, *Inorg. Chem.* 45 (2006) 2770.
- [3] W. Paw, S.D. Cummings, M.A. Mansour, W.B. Connick, D.K. Geiger, R. Eisenberg, *Coord. Chem. Rev.* 171 (1998) 125.
- [4] S.D. Cummings, R. Eisenberg, *J. Am. Chem. Soc.* 118 (1996) 1949.
- [5] C.R. Brodie, J.G. Collins, J.R. Aldrich-Wright, *J. Chem. Soc., Dalton Trans.* (2004) 1145.
- [6] J.V. Slageren, A. Klein, S. Zalis, *Coord. Chem. Rev.* 230 (2002) 193.
- [7] M. Hissler, J.E. McGarrah, W.B. Connick, D.K. Geiger, S.D. Cummings, R. Eisenberg, *Coord. Chem. Rev.* 208 (2000) 115.
- [8] V.M. Miskowski, V.H. Houlding, C.M. Che, Y. Wang, *Inorg. Chem.* 32 (1993) 2518.
- [9] R.H. Herber, M. Croft, M.J. Coyer, B. Bilash, A. Sahinert, *Inorg. Chem.* 33 (1994) 2422.
- [10] W.B. Connick, L.M. Henling, R.E. Marsh, H.B. Gray, *Inorg. Chem.* 35 (1996) 6261.
- [11] V.H. Houlding, V.M. Miskowski, *Coord. Chem. Rev.* 111 (1991) 145.
- [12] B.Z. Momeni, S. Hamzeh, S.S. Hosseini, F. Rominger, *Inorg. Chim. Acta* 360 (2007) 2661.
- [13] G.G. Friaza, A.F. Botello, J.M. Perez, M.J. Prieto, V. Moreno, *J. Inorg. Biochem.* 100 (2006) 1368.
- [14] M.L. Conrad, J.E. Enman, S.J. Scales, H. Zhang, C.M. Vogels, M.T. Saleh, A. Decken, S.A. Westcott, *Inorg. Chim. Acta* 358 (2005) 63.
- [15] B.P. Buffin, E.B. Fonger, A. Kundu, *Inorg. Chim. Acta* 355 (2003) 340.
- [16] J.A. Perez, J.n. Pons, X. Solans, M.F. Bardia, J. Ros, *Inorg. Chim. Acta* 358 (2005) 617.
- [17] X.F. He, C.M. Vogels, A. Decken, S.A. Westcott, *Polyhedron* 23 (2004) 155.
- [18] G.J.P. Britovsek, G.Y.Y. Woo, N. Assavathorn, *J. Organomet. Chem.* 679 (2003) 110.
- [19] D.D. Perrin, W.L. Armarego, D.R. Perrin, *Purification of Laboratory Chemicals*, second ed., Pergamon, New York, 1990.
- [20] F.P. Fanizzi, F.P. Intini, L. Maresca, G. Natile, *J. Chem. Soc., Dalton Trans.* (1990) 199.
- [21] S. Dehghanpour, A. Mahmoudi, *Main Group Chem.* 6 (2007) 121.
- [22] S.J. Scales, H. Zhang, P.A. Chapman, C.P. McRory, E.J. Derrah, C.M. Vogels, M.T. Saleh, A. Decken, S.A. Westcott, *Polyhedron* 23 (2004) 2169.
- [23] K. Kawakami, T. Ohara, G. Matsubayashi, T. Tanaka, *Bull. Chem. Soc. Jpn.* 48 (1975) 1440.
- [24] Z. Otwinowski, W. Minor, *Methods in enzymology*, in: C.W. Carter, R.M. Sweet (Eds.), *Macromolecular Crystallography, Part A*, vol. 276, Academic press, London, 1997.
- [25] R.H. Blessing, *Acta Crystallogr.* A51 (1995) 33.
- [26] G.M. Sheldrick, *Acta Crystallogr.* A64 (2008) 112.
- [27] K. Nakamoto, *Infrared and Raman Spectra of Inorganic and Coordination Complexes*, fourth ed., Wiley, New York, 1992.
- [28] E. Gabano, E. Marengo, M. Bobba, E. Robotti, C. Cassino, M. Botta, D. Osella, *Coord. Chem. Rev.* 250 (2006) 2158.
- [29] E. Pantoja, A. Gallipoli, S.V. Zutphen, D.M. Tooke, A.L. Spek, C.N. Ranninger, J. Reedijk, *Inorg. Chim. Acta* 359 (2006) 4335.
- [30] P.S. Pregosin, *Coord. Chem. Rev.* 44 (1982) 247.
- [31] P.S. Pregosin, *Transition Metal Nuclear Magnetic Resonance*, Elsevier, Zurich, Switzerland, 1991.
- [32] V. Anbalagan, R. Srinivasan, K.S. Kozarekar, S. Pallavi, *Transition Met. Chem.* 26 (2001) 603.
- [33] M. Martin, M.B. korgjerspersen, M. Hsu, J. Tewksbury, M. Laurent, K. Viswanath, H. Patterson, *Inorg. Chem.* 22 (1983) 647.
- [34] D. Collison, F.E. Mabbs, E.J.L. McInnes, K.J. Taylor, A.J. Welch, L.J. Yellowlees, *J. Chem. Soc., Dalton Trans.* (1996) 329.
- [35] E.J.L. McInnes, R.D. Farley, C.C. Rowlands, A.J. Welch, L. Rovatti, L.J. Yellowlees, *J. Chem. Soc., Dalton Trans.* (1999) 4203.
- [36] P.S. Braterman, J.I. Song, F.M. Wimmer, S. Wimmer, W. Kaim, A. Klein, R.D. Peacock, *Inorg. Chem.* 31 (1992) 5084.
- [37] T.V. Laine, U. Piironen, K. Lappalainen, M. Klinga, E. Aitola, M. Leskela, *J. Organomet. Chem.* 606 (2000) 112.
- [38] T.V. Laine, M. Klinga, M. Leskela, *Eur. J. Inorg. Chem.* (1999) 959.
- [39] A. Bacchi, M. Carcelli, C. Pelizzi, G. Pelizzi, P. Pelagatti, S. Ugoletti, *Eur. J. Inorg. Chem.* (2002) 2179.
- [40] R.S. Osborn, D. Rogers, *J. Chem. Soc., Dalton Trans.* (1974) 1002.
- [41] B.Z. Momeni, Z. Moradi, M. Rashidi, F. Rominger, *Polyhedron* 28 (2009) 381.